Research Article   **Open Access**

Dynamical Study for Selective Extreme Events over Iraq and their Relations with General Circulations

Ali. J. Mohammed*, Samir k. Mohammed, Jasim H. Kadhum

Department of Atmospheric Sciences, College of Science, Mustansiriyah University, Baghdad, IRAQ

*Correspondent contact: ali.alhafiz.atmsc@uomustansiriyah.edu.iq

ABSTRACT

The cold events and Precipitation conditions having special attention in the last years due to their impact on human health, ecosystems, and other aspects such as agriculture, hydrology. The ECMWF ERA-Interim 12-hourly (03 and 15 UTC) total precipitations and Tmin in a 1° x 1° grid covering Iraq, from 29° N to 38° N and from 39° W to 48° E, with a total of 10 by 10 cells, was used. At each grid point, extremes were defined as those events in which total precipitations were above 99th percentile for the 25 years period 1994-2018. For more investigation, the Hybrid Single-Particle Lagrangian Integrated The trajectory (HYSPLIT) model was used to study the dynamical mechanism that led to producing the cold events in Iraq. The number of extreme precipitations patterns shows an increasing behavior in the number of extreme events especially in the last decade, farther more there is a significant increase in the number of extreme precipitations in the last three years ago. No correlations were found with NAO, EA index, in contrast, there is a significant negative correlation with winter Arctic oscillations index. The aim of this work is studying the precipitation and cold extreme events in Iraq and their relations of most hemispheric pattern which influence in the Middle East region such as North Atlantic Oscillation (NAO), East Atlantic index (EA), Artic oscillation index (AO) and Mediterranean index (MOi). We speculate that the results of this study can provide a better understanding of extreme cold and precipitations anomalies in Iraq from a large-scale view.

KEYWORDS: Climate index; Cold events; Extreme; Precipitations.

الخلاصة

حظيت الأحداث الباردة و هطول الأمطار باهتمام خاص في السنوات الأخيرة بسبب تأثيرها على صحة الإنسان والنظم البيئية والجوانب الأخرى مثل الزراعة والهيدرولوجيا. تم استخدام بيانات المركز الاوربي ولمدة زمنية ١٢ ساعة للاوقات ١٣ و ١٥ بالتوقيت العالمي للهطول الكلي ودرجة الحرارة الصغرى باستخدام شبكة بيانات ١° x ١° تغطي كل العراق باحداثيات من ٢٩ درجة شمالاً إلى ٣٨ درجة شمالاً ومن ٣٩ درجة غربًا إلى ٤٨ درجة شرقًا، بإجمالي مساحة خلايا ١٠ في ١٠.في كل نقطة من نقاط الشبكة ، تم تعريف التطرف على أنه تلك الأحداث التي كان فيها إجمالي الترسبات أعلى من بنسبة ٩٩ في المئة لـ ٢٥ عامًا في الفترة ١٩٩٤-٢٠١٨. (لمزيد من الاستقصاء ، فان موديل the Hybrid Single-Particle Lagrangian Integrated Trajectory (HYSPLIT) تم استخدامه لدراسة الآلية الديناميكية التي أدت إلى إنتاج الأحداث الباردة فوق العراق. يُظهر عدد الأنماط الشديدة لهطول الأمطار سلوكًا متزايدًا في عدد الأحداث المتطرفة خاصةً في العقد الماضي ، والأكثر من ذلك أنه توجد زيادة ملحوظة في عدد احداث الهطول الشديد في السنوات الثلاث الماضية. وبالمقابل لم يتم العثور على ارتباطات مع NAO, EA index وهناك علاقة سلبية مع مؤشر تذبذبات القطب الشمالي الشتوي. نتوقع أن نتائج هذه الدراسة يمكن أن توفر فهمًا أفضل لحركةالانحرافات الشديدة للتساقط في العراق من منظور واسع النطاق. الهدف من هذا العمل هو دراسة هطول الأمطار والظواهر الباردة المتطرفة في العراق حيث تمت دراسة الأحداث وعلاقاتها في معظم أنماط نصف الكرة الشمالي التي تؤثر في منطقة الشرق الأوسط مثل North Atlantic Oscillation (NAO), East Atlantic index (EA), Artic oscillation index (AO) and Mediterranean index (MOi).

INTRODUCTION

Iraq has an arid climate and extreme temperatures are frequent in winter and summer. Despite Iraq has been listed as one of the most vulnerable countries to climate change in the Arab region [1], few works have studied the underlying phenomena that cause extreme temperatures at the region. Robaa and Al-Barzanji 2015 [2] evaluated the trends of surface air temperatures, Muslih and Błażejczyk 2016 [3] estimated the inter-annual changes and the long-term trends of monthly temperature .Furthermore, Salman et al 2017 [4] assessed the trends in annual and seasonal daily average minimum and maximum temperatures.

Regarding the relation between the extremes in Iraq and the large-scale circulation modes, Salar *et al.* 2015 [5] analysed the relation between circulation patterns leading to extreme events and hemispheric oscillation patterns, such as the North Atlantic Oscillation (NAO). They concluded that NAO positive phases causes the expansion of the desert climatic region (Bwh) and, simultaneously, diminishes the surface of other climate regions (BSH and Csa). In contrast, few studies analysed the relationship between cold events and the East Atlantic Index (EA) in eastern Mediterranean Sea and Iraq but Dragan-Burić *et al.* 2018 [6] find a link between EA index and changes of air temperature over the western Mediterranean Sea. However, the synoptic and mesoscale conditions and the dynamics of the air masses causing the extreme temperatures have not been addressed yet.

On the east side of the Mediterranean Sea, Iraq is located in southwest Asia (lat: 29°15′N–38°15′N and long: 38°45–48°45′E) in the northern temperate zone, but with continental and subtropical climate characteristics. Most of the Iraq surface is mainly of lowlands that do not exceed 300 m of altitude. Three major geographic regions can be identified: desert in the west and southwest, extending uplands between the Euphrates and Tigris rivers; mountains in the north and northeast; and alluvial lowland in the central and southern regions. In northern Iraq, mountains located E-W rise to over 3600 m near the Turkish and Iranian borders including the Taurus Mountains near Turkey and the Zagros Mountains that lie across the border in Iran [7]. The annual mean maximum temperature range is 41 - 48 ℃, in summer; especially hot are the central and southern regions. The annual mean minimum temperatures reach the freezing point in the north and stay around 5°C in the southern area [4].

Most of the precipitation occurs during January and March. Mean monthly precipitation varies between 102-229 mm in northern Iraq, while in the center and the southern regions are varies between 25-76 mm. The south-western side of Iraq has the lowest mean amounts; 2.5 mm isolated, windward mountain sites have annual averages of 508 mm. In general, the annual average precipitation in Iraq is about 120 mm, which is less than 15% of the average rainfall in the world (860 mm) [8].

The persistent large-scale circulation patterns associated with the production of extreme temperatures in Europe is known to interfere with hemispheric oscillation patterns, in particular, North Atlantic Oscillation (NAO) and Arctic Oscillation (AO). The anomalous cold winter of 2010 was found to be strongly linked to a negative phase of the NAO [5, 9, 10, 11].

At the east of the Mediterranean Sea cold extreme events and precipitation are also influenced by hemispheric oscillation patterns, particularly the NAO, the AO and the EA. In Iraq, Al Khalid et al 2017 [9] found a relationship between the positive phase of NAO and temperature anomalies in winter. These anomalies are caused by the westerly advection of warm air over the Middle East which extends from north of Africa and through the northeast of Iraq. Also, Salar *et al.* 2015 [5], cconcluded that NAO positive phase causes an expansion of the desert climatic region and simultaneous diminishes the surface of the other climate regions. On the other hand, little attention has been devoted to the impact of EA in the Middle East climate despite it is one of the most important patterns characterizing the extratropical climate variability in the Northern Hemisphere [12].

The Iraqi region has a climate similar to that of the Eastern Mediterranean (EM) region, characterized by rainy winters and dry and hot summers. Therefore, the foremost influential synoptic systems in the meteorology of the EM are the subtropical high-pressure system, the winter Siberian anticyclone, the monsoon low pressure, the Red Sea trough and the Mediterranean low (extra-tropical low) [13].

This paper is focused on the study of the cold extreme and precipitation episodes in Iraq for a period of 25 years (1994-2018), based on the 12-hous minimum temperatures at 2-m height and total precipitation obtained from the ECMWF ERA-Interim reanalysis database. The characterization of the cold extremes has been done by means of: 1) a Lagrangian method to study the air mass pathways; 2) the study of the physical variables evolution along the back trajectories.

MATERIALS AND METHODOLOGY

The following data was used: ECMWF ERA-Interim 12-hourly (03 and 15 UTC) 2m lowest temperature data (T_{min}) and total precipitation

covering Iraq (from 29° N to 38° N and from 39° E to 48° E, with a grid of 10×10 cells). At each grid point, cold extremes were defined as events where T_{min} was below the 0.1th percentile for the 25-years period. Where the total precipitation was defining above 99th percentile for the 25-years period. The operation yielded 19 cold extremes at each grid point; a total of 1900 cold extreme events over 100 grid points were recorded in Iraq. The persistence of extreme events was analyzed separately for diurnal (15 UTC) and nocturnal (03 UTC) extremes by applying the criterion of the 0.1th percentile to the T_{min} data.

1. Correlations with climatic indice

The North Atlantic Oscillation (NAO indices) [13], Mediterranean Oscillation Indices MOi; Artic oscillations (AO; National Oceanic and Atmospheric Administration (NOAA)/National Center for Environmental Prediction (NCEP), Climate Prediction Center), and East Atlantic indices (EA), (NOAA)/NCEP, Climate Prediction Center) were correlated with the annual number of extremes and the annual extreme temperature average. Standardized data (obtained by subtracting the mean and dividing by the standard deviation) are used for the extremes and the climatic indices. The Spearman rank correlation coefficient, the Kendall-tau, and the Pearson coefficient are computed the relationship between precipitation/cold extremes events and climatic index.

2. Trajectory model

A Lagrangian method was used to comput the backward trajectories to identify the origin and pathway of the precipitation/cold extreme air-masses. The Hybrid Single-Particle Lagrangian Integrated Trajectory (HYSPLIT) model was used here. HYSPLIT was developed by the Air Resources Laboratory (ARL) of the NOAA; it received an upgrade in 2001 by NOAA and the Australian Bureau of Meteorology [14]. The representation of trajectory densities, i.e. the number of time steps per grid box at different levels, is used to identify source areas of air masses. Densities are computed for the back-trajectories of 4- and 10-days length associated to hot and cold extreme events at the levels of 100 and 1500 m. The domains used for the trajectory density representation is given by the coordinates: 00ºE-74ºE to 00ºN-59ºN for Iraq. The maps of trajectory densities help to determine the meridional and horizontal advection development during the extremes, and the median and average length of the back-trajectories.

3. Physical variables along the trajectories

In order to understand the air masses dynamics that leading to produce the cold extreme events, a set of variables was tracking along with the back-trajectories: height, pressure, temperature, relative humidity, downward solar radiation, potential temperature, flux mixing-layer height, latitude and longitude Table .1. These variables determine the height and location of the air mass at a specific time step, as well as its thermodynamic properties: temperature changes caused by heating/cooling during diabatic/adiabatic vertical displacements, radiative processes, humidity changes and surface heat fluxes. In order to provide a measure of the deviance of an air-mass property from its final state, their evolution along the back-trajectories were analyzed in terms of differences regarding their final value at the grid point, except for mixing-layer height and downward solar radiation. To follow the temporal changes, five percentiles of the variables were traced along the trajectories: the median 50th, the upper and lower quartiles 75th and 25th and the 5th and 95th percentiles. The physical variables are obtained as an optional output of HYSPLIT. The data is retrieved from the Global Forecast System (GFS) model and interpolated to the coarser grid of the trajectories.

Table 1. Physical variables used in monitoring extreme events.

Variable	Symbol [Units]
Pressure	P [hPa]
Temperature	T [°C]
Potential Temperature	θ [K]
Relative Humidity	RH [%]
Downward Solar Radiation Flux	DSR [Wm^{-2}]
Mixing-Layer Depth	MLD [m]

RESULTS AND DISCUSSION

## Annual distribution and correlation with climatic indices

Regarding the cold events, Fig.1 a shows the average temperature of cold extremes at each grid point. The lowest values for the cold events correspond to the NE region and the highest ones to the S, with a difference between them of about 25 K. in contrast , Fig 1b shows the total precipitation at each grid point, the lowest value was recorded in the Sw and W part of Iraq with 0.008 m were the highest value was recorded in N and E part with 0.062m. These results are corresponding with al Al-Salihi *et al* 2013[8] results which found the same amount of rainfall over Iraq.

The Spearman rank, Kendall's tau and the Pearson's correlation were applied for detecting correlations between the annual and winter climatic indices (NAO, AO, Moi and EA) and the number of extreme events. In contrast, a significant positive correlation ($p<0.01$) were found between the annual cold average temperature and positive phase of the EA pattern (Kendall: -0.385; Spearman: 0.531; and Pearson: 0.525). This result differs from Al Khalid et al 2017[9] who found a relationship between the positive phase of NAO and temperature anomalies in winter over Iraq during the period 1979-2016, probably due to the different length of the analysed periods.

Regarding the total perception, no correlations were found with NAO, AO, MOi and EA indices. On the other hand, a significant negative correlation ($p<0.01$) was found between the number of extreme perceptions and the winter positive phase of the AO pattern (Kendall: -0.284; Spearman: -0.400).

a

b
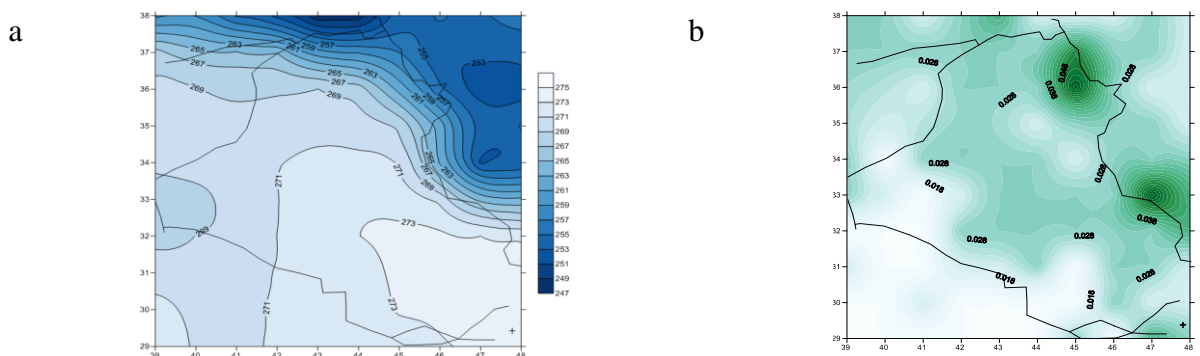
Figure 1. Geographical distribution of the a) average of cold extreme events temperatures at each grid point for the 25-year period and b) total precipitation at each grid point for the 25-year period.

Regarding the evolution of the number of cold over the period 1994-2018 Fig.2a, 67% of the events occurred during the second decade. In all regions there are important peaks in the number of cold events in 1994, 1997 and 2008, representing 57% of the total number of events. All regions show an exceptional peak during the winters of 1997 and 2008. From 2009 to 2018,

all regions registered a decrease in the number of cold events – except in 2016 and 2017. The general trend of the number of cold events for all regions is positive: 13 days/decade.

On the other hand, the evolution of the number of perceptions events over the period 1994-2018 Fig.2b, 40% of the events occurred during the first decade.

a

b
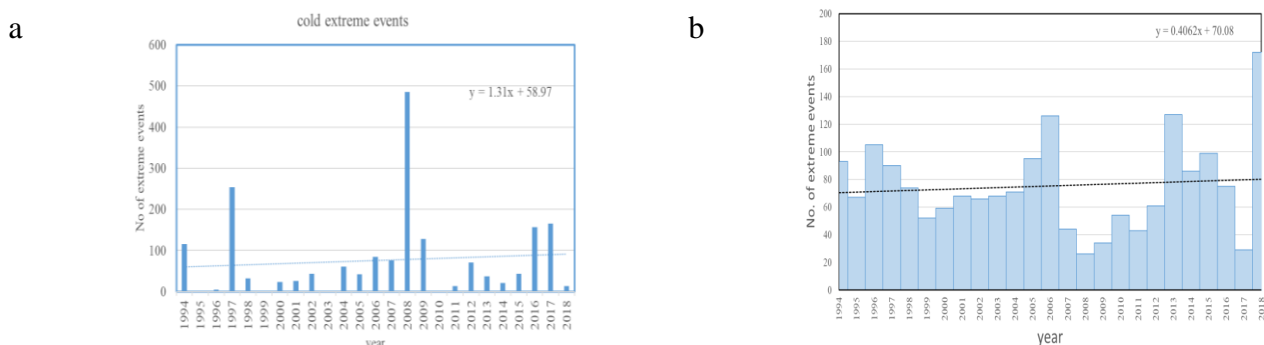
Figure 2. Annual number of extreme events for Iraq, showing a) cold events, and b) precipitation events at each grid point for the 25-year period. The dashed lines represent the tendency for Iraq.

In all regions there are important peaks in the number of precipitation events in 1996 ,2008, 2013 and 2018 representing 30% of the total number of events. All regions show an exceptional peak during the winters of 2013 and 2018. From 2009 to 2018, all regions registered an increases in the number of perceptions events – except in 2017. The general trend of the number of perceptions events for all regions is positive: 4 days/decade.

Trajectory densities
Back-trajectories were computed using the coordinates of the grid points as final destination at the time the episodes occurred. For the cold events, the distance travelled by the median is 1325 km and 2740 km at 100 and 1500 m a.s.l., respectively. For 10-day back-trajectories, these distances are 2500 km at 100 m and 2220 km at 1500 m a.s.l. for hot events,

and 3900 km and 6570 km for cold events. Cold-event trajectories are faster probably because are related to advection processes. The trajectory densities, i.e., the number of back-trajectory time steps per grid box (1°×1°) were calculated by superimposing a grid mesh of 1°×1° to the integration domain of the back-trajectories. Densities were computed for 4- and 10-day back-trajectories, at 100 and 1500 m a.s.l. Figures 3a and b shows the density of 4-days back-trajectories at 100 m and 1500 m a.s.l. for the cold events, the distribution of densities is similar for the 10-days back-trajectories (Figs. 3c and d), and indicates that the main flow is from East Europe and Siberia, travelling over the Black Sea at low levels, while it shifts more to the north-west at high levels.
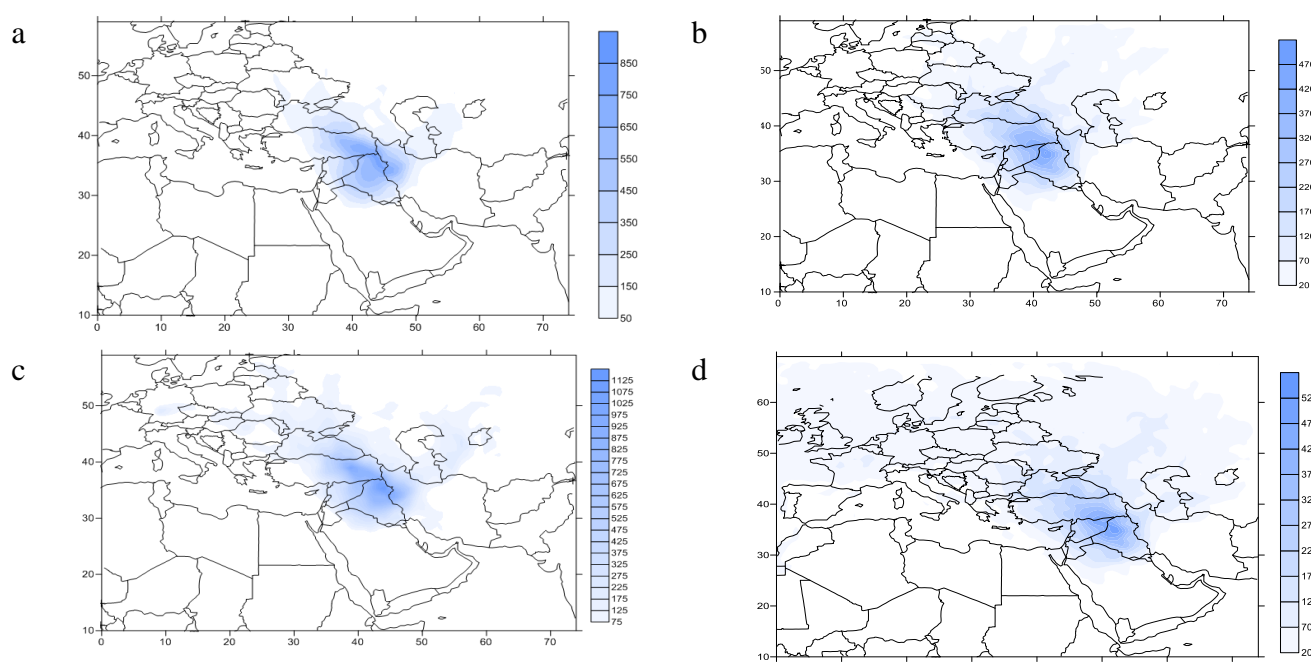

Figure 3. Trajectory densities (number of time steps per grid box) during cold extremes for 4-days back-trajectories at a) 100 m, b) 1500 m; and 10-days back-trajectories at c) 100 m, d) 1500 m height.

As mentioned above, the meridional and zonal displacements of the cold air masses along the trajectories are greater than for the hot air masses. Figs 4 a, b shows the evolution of latitude and longitude for the 5th, 25th, 50th, 75th and 95th percentiles for the back-trajectories arriving at 100 m and producing a cold extreme event. The longitudinal and latitudinal differences for the median are about 20 degrees during the 10 days, indicating advection of cold air masses from the

Siberian regions and Europe. The latitudinal shift takes place mainly over the six days before the cold events Fig.4 a. This result is proportionate with situations in which large blocking anticyclone over the Siberian region and North-western Russia drives easterly winds over Europe and Middle East. This was identified as an important synoptic-scale cause of winter cold spells by Wallace *et al*. 2006[11] and Ghanghermeh *et al*. 2015 [12]. Fig 4 c shows how

67

the median air mass pathway starts over Belarus and moves to Ukraine, and pass the Black see toured to Turkey, before entering Iraq from the north, 40 hours before the extreme events. Finally, it moves to Central Iraq.
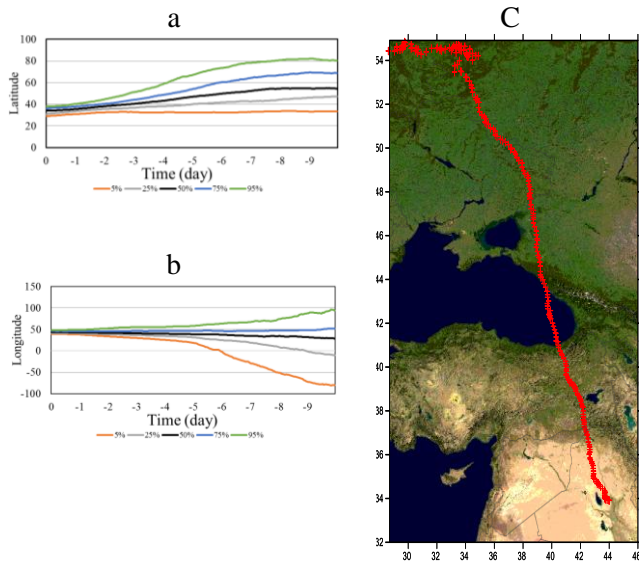
Figure 4. a) Meridional and b) zonal evolution of the 5th, 25th, 50th, 75th and 95th percentiles along the 100 m height back-trajectories of the air-masses causing cold extreme events in Iraq and c) median pathway.

Evolution of the physical variables for cold events

Fig. 5 shows the evolution of potential temperature, temperature, , relative humidity, mixing-layer height and downward solar radiation along the 5th, 25th, 50th, 75th and 95th percentiles of 10-day back-trajectories for the cold events. Temperature shows moderate diurnal cycle more pronounced during the days previous to the extreme events. There is a progressive increase of temperature as the air mass approaches Iraq: +28 K and +5 K for the 5th and 95th percentiles, respectively and +9 K for the median Fig.5a. Median potential temperature Fig. 5b shows a different evolution and consequently diabetic and adiabatic processes are involved during the median trajectory. Only during the last 14 hours before the event both temperatures present a similar evolution due to a diabetic process involving radiative cooling during the night once the air mass has entered Iraq.
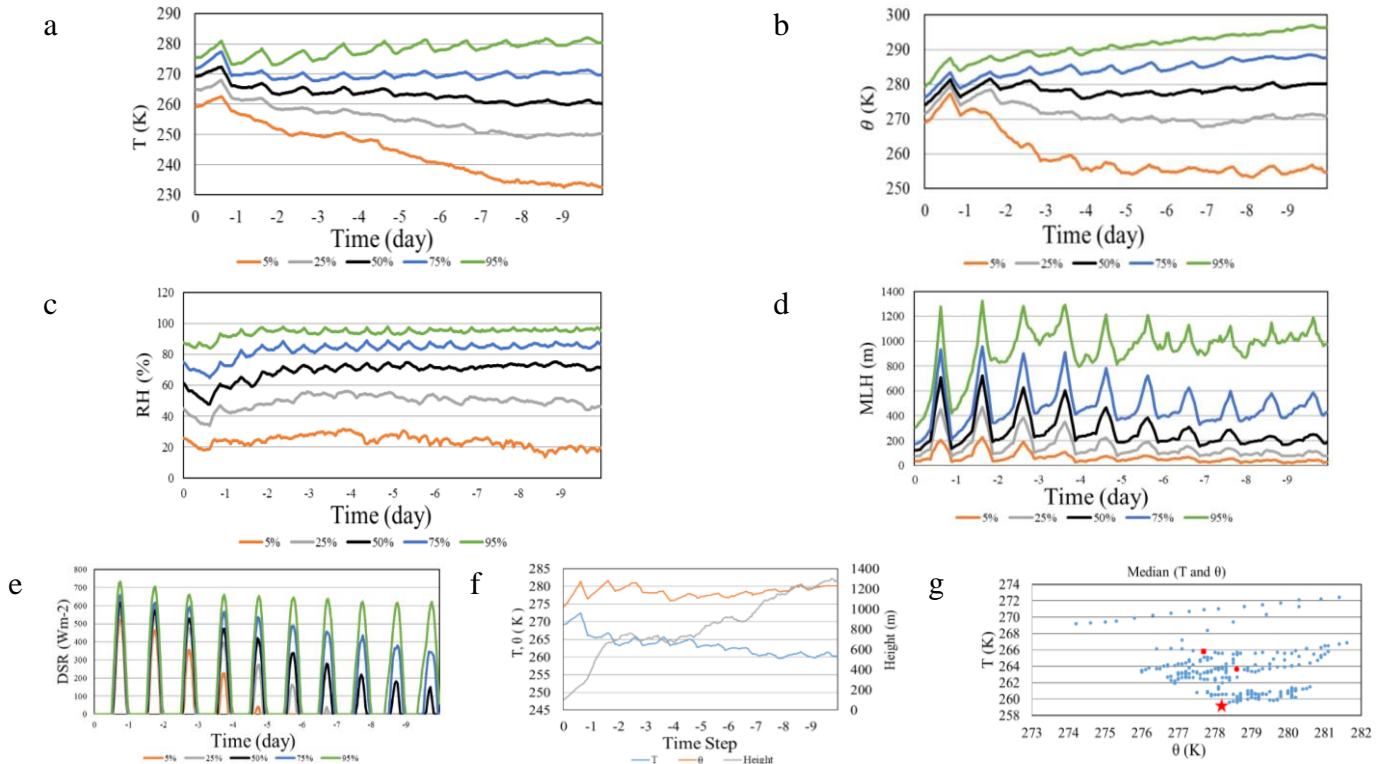
Figure 5. Evolution along the back-trajectories of cold events of the 5th, 25th, 50th, 75th and 95th percentiles of a) temperature; b) potential temperature; c) mixing-layer height; d) relative humidity, e) downward solar radiation, f) median temperature, potential temperature and height and g) temperature vs potential temperature along the 10-days back-trajectories at 100 m for cold extremes. Each point represents the T and θ median of all trajectories at a specific time step. The star indicates the beginning of the trajectory 10 days before the extreme events, the blue circle 72 hours before and the red square 24 hours before extreme event.

The evolution of the mixing-layer height shows a less-pronounced diurnal cycle than for the warm extremes Fig. 5c. From day 10 to 6 before the events, the mixing-layer height oscillation is almost imperceptible for the median and the values are lower. During these days the air mass is at high latitudes. Diurnal oscillation became more pronounced five days prior to the events, whereas higher values occur when the air mass travels over Turkey and it enters in Iraq.

In contrast to hot events, the median incident solar radiation flux for cold events displayed low values when the air mass is at high latitudes (days 10 to 9). Then it progressively increases as the air mass moves south, reflecting the large difference of incoming solar radiation during the winter between places with different latitude Fig. 5d.

Relative humidity of the median trajectory shows large values remaining relatively constant over the central part of the path when the air mass crosses over continental Europe, followed by an increase the day prior to the events Fig. 5e due to inverse relationship between the temperature and relative humidity.

The evolution of temperature and potential temperature along the median back-trajectory Fig. 5f reflects the diurnal cycle of radiative heating/cooling, that is amplified as the air-masses approaches their destination in Iraq. Diabatic heating during the diurnal hours by absorption of sensible heat from the surface is particularly important during the last two days, as well as the radiative cooling during night of the last 12 hours. On the other hand, subsidence is present in the entire path Fig. 5g. Thus, an important contribution to the global temperature increase of 9 K is due to adiabatic warming by descent of the air masses. During the first three days in which the air masses move over high-latitudinal regions radiative cooling is compensated by adiabatic warming and the temperature remain approximately constant. Afterwards, a net increase in temperature is produced probably because the cooling is lower as the air masses cross regions of lower latitude, prevailing adiabatic warming.

The evolution of the back-trajectories and the associated physical variables indicates that cold events are caused by this mechanism: air mass advection from Siberia and Eastern Europe seems to be the main process that causes cold extreme events. This is in agreement with the presence of Siberian high-pressure systems centered over Turkey, covering most of the eastern Mediterranean and bringing cold air to Iraq, described by Ghanghermeh *et al*. 2015 [12].

CONCLUSION

A Lagrangian approach is used to investigate the driving mechanisms of cold extreme events over a 25-year period (1994-2018) in Iraq, based on the 0.1^{th} percentile of the 2-m lowest temperature and 90th percentile profiles of the ERA-Interim reanalysis data.

We find a positive trend in the number of both cold and perceptions events during the analysed period.

Concerning the influence of primary climatic patterns affecting the Middle East, the average temperature of cold extremes correlated positively ($p<0.01$) with EA. In contrast, no correlations with NAO, Moi and AO indices were obtained for cold extreme events, On the other hand, no correlations were found for events.

The back-trajectories of cold events are associated to advection of air masses from Siberia and north-eastern Europe. The evolution of the median temperature versus the median potential temperature shows that air masses experience radiative cooling during their passage over the northern regions that is approximately balanced by adiabatic heating associated with the descend of the air masses. Adiabatic warming due to subsidence prevails during the last days, and is persistent until the start of the episodes.

REFERENCES

[1] UNDP, Elasha, B.O. Mapping of climate change threats and human development impacts in the Arab region. In: UNDP Arab Development Report–Research Paper Series. UNDP Regiona Bureau for the Arab States., (2010).

[2] Robaa ES, Al-Barazanji Z. Mann-Kendall trend analysis of surface air temperatures and rainfall in Iraq. Idojaras. 2015 Oct 1;119(4):493-514.

[3] Muslih KD, Błażejczyk K. The inter-annual variations and the long-term trends of monthly air temperatures in Iraq over the period 1941–2013. Theor Appl Climatol. 2017 Oct 1;130(1-2):583-96.

[4] Salman SA, Shahid S, Ismail T, Chung ES, Al-Abadi AM. Long-term trends in daily temperature extremes in Iraq. Atmos Res. 2017 Dec 1;198:97-107.

[5] Khidher SA, Pilesjö P. The effect of the North Atlantic Oscillation on the Iraqi climate 1982–2000. Theor Appl Climatol. 2015 Nov 1;122(3-4):771-82.

[6] Burić DB, Dragojlović JM, Milenković MÐ, Popović LZ, Doderović MM. Influence of variability of the East

Atlantic Oscillation on the air temperature in Montenegro. Thermal Science. 2018; 22(1 Part B):759-66.

[7]   Malinowski JC (2003) Iraq geography, west point. United States Military Academy, New York, first edition:29-37

[8]   Al-Salihi AM, Al-Lami AM, Mohammed AJ. Prediction of monthly rainfall for selected meteorological stations in Iraq using back propagation algorithms. J Environ Sci Technol. 2013 Jan 1;6(1):16-28.

[9]   Al-Khalidi J, Dima M, Vaideanu P, Stefan S. North Atlantic and Indian Ocean links with Iraq Climate. Atmosphere (Basel). 2017 Dec;8(12):235.

[10] Favà V, Curto JJ, Llasat MC. Relationship between the summer NAO and maximum temperatures for the Iberian Peninsula. Theor Appl Climatol. 2016 Oct 1;126(1-2):77-91.

[11] Rodrigo FS. On the covariability of seasonal temperature and precipitation in Spain, 1956–2005. Int J Climatol. 2015 Sep;35(11):3362-70

[12] Wallace JM, Hobbs PV. Atmospheric science: an introductory survey. Elsevier; 2006 Mar 24. second editions,6:252-290

[13] Ghanghermeh AA, Roshan GR, Shahkooeei E. Evaluation of the effect of Siberia's high pressure extension on daily minimum temperature changes in Iran. Model Earth Syst Environ. 2015 Oct 1;1(3):20.

[14] Wallace JM, Gutzler DS. Teleconnections in the geopotential height field during the Northern Hemisphere winter. Mon. Weather Rev. 1981 Apr;109(4):784-812.

[15] Draxler RR, Hess GD. An overview of the HYSPLIT_4 modelling system for trajectories. Aust Met Mag.1998 Dec;47(4):295-308.